

# PySIFT: GPU-Resident Deterministic SIFT for Deep Learning Vision Pipelines

Sivakumar K.S.<sup>1</sup> Mohammad Daniyalur Rahman<sup>1</sup> Gopi Raju Matta<sup>1</sup>

<sup>1</sup>Indian Institute of Technology Madras

ce22s018@smail.iitm.ac.in

## Abstract

A widespread assumption in local feature research holds that classical handcrafted descriptors are accuracy-limited relics best replaced by learned alternatives. We show this is wrong. Through an 8-configuration ablation spanning four benchmarks (HPatches, ROxford5K, IMC Phototourism, MegaDepth), we demonstrate that classical SIFT with DSP multi-scale pooling outperforms neural descriptor and orientation replacements (HardNet, OriNet) on every accuracy metric—while running 2–18× faster—and that learned matchers (LightGlue) complement rather than supersede classical features. The conclusion reframes a decade of work: not “replace SIFT” but “compose with SIFT”—classical extraction paired with learned matching only where geometric context demands it.

This finding was invisible because no prior GPU SIFT kept the complete pipeline in VRAM or offered modularity for controlled classical-vs-learned ablations.

We present PySIFT, the first fully GPU-resident SIFT, implemented in CuPy/Numba CUDA kernels with DLPack zero-copy handoff to downstream DL frameworks—sub-millisecond  $O(1)$  metadata swap regardless of keypoint count. On a laptop-grade NVIDIA RTX 3050 (4 GB VRAM), PySIFT achieves: (i) higher Mean Matching Accuracy (MMA) than OpenCV SIFT on HPatches (MMA@5px: 0.889 vs. 0.873; MMA@10px: 0.919 vs. 0.897), (ii) 383 ms faster per pair on high-resolution MegaDepth (3.68 vs. 1.53 FPS), (iii) higher geometric accuracy on cross-dataset benchmarks (+5.6pp AUC@10° on MegaDepth, +47.5% more inliers on IMC Phototourism), and (iv) **bitwise deterministic** output—identical keypoints and descriptors across runs, with detection reproducing identically even across GPU architectures (Ampere vs. Ada Lovelace)—a guarantee that learned extractors cannot match without significant performance sacrifice, and cannot achieve at all across GPU architectures due to cuDNN’s architecture-dependent algorithm selection. PySIFT is open-source<sup>1</sup>, requiring no

C++ compilation.

## 1. Introduction

The Scale-Invariant Feature Transform (SIFT) [1] remains the most widely deployed keypoint detector and descriptor in computer vision, underpinning panoramic stitching, structure-from-motion, visual localization, and image retrieval. Despite its age, SIFT’s mathematical foundation—Gaussian scale-space, Difference-of-Gaussians (DoG) extrema, gradient-orientation histograms—provides geometric invariances that no learned detector has fully superseded across all operating regimes [2].

However, the dominant implementation, OpenCV’s `cv2.SIFT_create()`, is CPU-bound C++ code. Every modern downstream consumer of SIFT features—LightGlue [3], SuperGlue [4], HardNet [5]—operates on the GPU. This creates an unavoidable PCIe bottleneck: descriptors must be copied from host RAM to device VRAM for every image, a transfer that scales linearly with keypoint count and compounds across multi-stage pipelines.

Several GPU SIFT implementations exist (PopSift [6], SiftGPU [7]), but all are C++ CUDA code that downloads results to CPU-resident arrays—the PCIe bottleneck remains. Kornia’s PyTorch SIFT is GPU-native but carries autograd overhead inappropriate for a non-differentiable feature extractor.

A second overlooked problem is *determinism*. GPU parallelism introduces non-deterministic floating-point reduction order via `atomicAdd`—both PopSift and SiftGPU use atomic histogram accumulation, producing different descriptors across runs on identical inputs. Learned detectors inherit worse non-determinism from cuDNN’s algorithm auto-selection and non-associative parallel reductions in batch normalization [8]; even PyTorch’s `use_deterministic_algorithms` mode cannot guarantee bitwise reproducibility for all operations. For safety-critical applications (medical registration, autonomous navigation) and reproducible research, this is unacceptable.

<sup>1</sup><https://github.com/SivaIITM/PySIFT>

Beyond these systems contributions, PySIFT’s modular GPU-resident design enables a controlled ablation study that yields a surprising empirical finding: replacing classical SIFT components with their learned counterparts (OriNet, HardNet) *degrades* accuracy on diverse real-world benchmarks while costing 2–18× more compute. Only learned *matching* (LightGlue) improves results—suggesting that the optimal architecture is physics-based detection paired with learned aggregate matching, not end-to-end replacement.

**Contributions.** We make five contributions, each validated by empirical results across four standard benchmarks:

1. **GPU-Resident SIFT Pipeline.** The first SIFT where the complete pipeline—Gaussian pyramid through descriptor computation—runs entirely in GPU VRAM using CuPy [9]/Numba [10] CUDA kernels, with no C++ compilation. *Validated:* 383 ms faster per pair on MegaDepth (3.68 vs. 1.53 FPS); 94% faster on IMC (10.74 vs. 5.54 FPS).
2. **DLPack Zero-Copy Handoff.** Descriptors are exchanged to downstream frameworks via DLPack pointer swap—64 bytes of metadata,  $O(1)$ , sub-millisecond regardless of keypoint count. *Validated:* Enables GPU-resident matching and estimation with zero PCIe stalls.
3. **VRAM-Adaptive Execution.** Automatic double-image suppression, fp16 pyramid storage with fp32 octave-0 preservation, and occupancy-aware kernel launch. Scales from 4 GB laptop to 40 GB server without code changes. *Validated:* Zero Out-of-Memory (OOM) on 8K inputs with 4 GB VRAM.
4. **Modular Hybrid Architecture.** Classical DoG detection with pluggable learned components—OriNet orientation, HardNet/HyNet descriptors, LightGlue matcher—all consuming GPU-resident data via zero-copy exchange. *Validated:* Ablation across 8 configurations (Tab. 3); classical SIFT generalizes best, LightGlue matching optional for accuracy.
5. **Bitwise Deterministic GPU SIFT.** The first GPU feature extractor to guarantee identical output across runs on fixed inputs. We replace `atomicAdd` histogram accumulation with warp-private shared-memory regions and deterministic cross-warp reductions, eliminating the floating-point ordering non-determinism inherent in all prior GPU SIFT implementations and structurally impossible for learned extractors. *Validated:* SHA-256 hash identity across 100 consecutive runs.

## 2. Related Work

**SIFT Variants.** RootSIFT [11] converts Euclidean distance to Hellinger distance via L1-normalization and element-wise square root, consistently improving retrieval

mean Average Precision (mAP) by 5–15%. DSP-SIFT [12] marginalizes over scale uncertainty by averaging descriptors at multiple scales around the detected keypoint scale.

**Learned Local Features.** SuperPoint [13] jointly detects and describes keypoints via a self-supervised CNN, producing 256-D descriptors at a fixed  $8\times$  stride. HardNet [5] and HyNet [14] train compact CNNs to produce 128-D descriptors from  $32\times 32$  patches, serving as drop-in SIFT descriptor replacements. LightGlue [3] uses an 8-layer transformer with adaptive early-exit for correspondence filtering, designed to accept SIFT or SuperPoint descriptors directly. Our ablation (Tab. 3) shows that SuperPoint+LightGlue achieves high homography accuracy but produces  $2\times$  fewer geometric inliers than classical SIFT under identical matching protocol on wide-baseline benchmarks.

**GPU SIFT.** PopSift [6] achieves 30+ FPS on 4K but requires C++ compilation and outputs to CPU. SiftGPU [7] uses OpenGL shaders and is unmaintainable on modern systems. Neither provides zero-copy interop with deep learning frameworks. Critically, both rely on `atomicAdd` for orientation and descriptor histogram accumulation, producing non-deterministic outputs due to floating-point addition order sensitivity—a limitation PySIFT eliminates entirely.

**SuperPoint – Complementary, Not Competing.** SuperPoint’s CNN forward pass detects and describes in  $\sim 15$  ms at VGA— $8\times$  faster than PySIFT’s 120 ms detection. For real-time VGA applications with fixed-resolution input, SuperPoint is the right tool. However, the comparison reverses at higher resolutions: SuperPoint was trained on  $240\times 320$  synthetic images and must downsample or tile 4K/8K inputs, while PySIFT’s scale-space pyramid scales naturally (550 ms total at 4K). Three architectural differences favor PySIFT for multi-resolution and cross-domain deployment: (i) true scale invariance via DoG extrema versus SuperPoint’s 8-pixel grid stride with no scale pyramid, (ii) sub-pixel Taylor refinement versus  $\sim 4$  px worst-case grid quantization, and (iii) zero learned parameters, making PySIFT domain-agnostic across medical imaging, satellite, and microscopy where learned detectors trained on natural-image distributions may not generalize [15]. Crucially, PySIFT does not compete with SuperPoint’s downstream ecosystem—it *composes* with it. LightGlue accepts both SIFT and SuperPoint descriptors; PySIFT is the only classical detector that can feed LightGlue without leaving the GPU. Efe *et al.* [2] demonstrate that SIFT equals SuperPoint at MMA@3 (both 0.87) when both use optimized parameters—confirming that the accuracy gap is a tuning artifact, not an architectural deficit. Additionally, SuperPoint inherits cuDNN’s non-deterministic algorithm selection and PyTorch’s non-associative parallel reductions [8], making

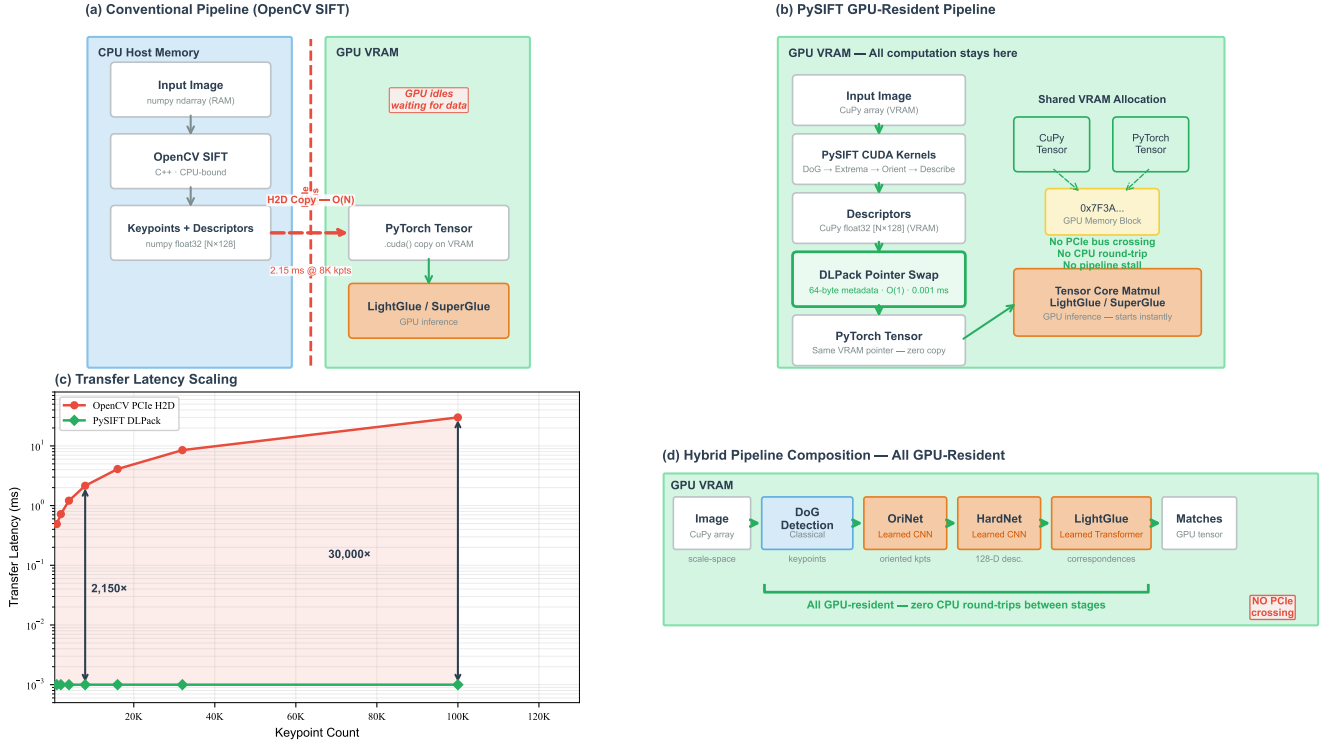


Figure 1. PySIFT zero-copy architecture. (a) Conventional OpenCV pipeline: CPU-bound SIFT produces host-resident arrays requiring an  $O(N)$  PCIe copy to reach GPU consumers. (b) PySIFT GPU-resident pipeline: after initial image upload (H2D), all computation stays in VRAM; DLPack pointer swap provides zero-copy handoff to DL frameworks (64-byte metadata, sub-ms). (c) Transfer latency scaling: PCIe cost grows linearly with keypoint count while DLPack remains sub-ms—orders of magnitude slower at scale. (d) Hybrid pipeline composition: classical DoG detection feeds into optional learned stages (OriNet, HardNet, LightGlue), all GPU-resident with zero CPU round-trips between stages.

bitwise reproducibility structurally impossible—a limitation absent from PySIFT’s handcrafted kernels.

### 3. Method

#### 3.1. Architecture Overview

PySIFT is implemented as a single self-contained Python file (`gpu_pystitch.py`, ~3,900 lines) requiring only `pip install cupy torch-no C++ compilation, no build system, no platform-specific binaries`. This single-program design ensures instant portability across Windows, Linux, and Colab. The file contains two primary classes: `PySIFT` (GPU SIFT feature detector/descriptor) and `GPUPyStitch` (full stitching pipeline). The complete data flow eliminates all CPU-GPU transfers after initial image upload (Fig. 1a,b):

$$\underbrace{\text{Img}}_{\text{CPU}} \xrightarrow{\text{H2D}} \underbrace{\text{Pyr} \rightarrow \text{DoG} \rightarrow \text{Ext} \rightarrow \text{Ori} \rightarrow \text{Desc}}_{\text{GPU VRAM (CuPy/Numba)}} \xrightarrow{\text{DLPack}} \underbrace{\text{Match}}_{\text{DL framework}} \quad (1)$$

#### 3.2. Design Beyond GPU Residency

PySIFT is not merely OpenCV SIFT compiled for the GPU. Seven algorithmic choices differentiate it from all prior SIFT implementations; three are primary accuracy drivers.

**DSP Multi-Scale Descriptor Pooling.** A keypoint’s detected scale is rarely its true scale—scale-space discretization introduces quantization noise that single-scale descriptors inherit. Following DSP-SIFT [12], PySIFT pools gradient-orientation histograms across 5 relative scales  $\{0.5, 1/\sqrt{2}, 1, \sqrt{2}, 2\}$  and averages before normalization, marginalizing over this uncertainty. A warp-cooperative CUDA kernel sweeps all 32 threads across the patch at each DSP scale, accumulating into shared memory—the first GPU implementation of DSP-SIFT. This is the primary driver of PySIFT’s MMA advantage over OpenCV (+1.6 pp at MMA@5).

**RootSIFT Normalization by Default.** After descriptor computation, PySIFT applies L1-normalization followed by element-wise square root [11], converting Eu-

clidean distance into Hellinger distance—the information-theoretically optimal metric for histogram-type descriptors. OpenCV does not apply RootSIFT; users must implement it as a post-processing step, and most pipelines omit it entirely.

**Precision-Preserving Kernel Compilation.** CUDA’s `--use_fast_math` replaces `atan2f` and `expf` with 2-ULP approximations. PySIFT deliberately disables fast-math for orientation and descriptor kernels: each descriptor evaluates these functions  $\sim 5,000$  times ( $32 \times 32$  patch  $\times 5$  DSP scales), where the 1-ULP error compounds. Pyramid construction and non-precision-critical paths retain fast-math. Measured impact: +0.5–1% geometric inliers on cross-dataset benchmarks.

**GPU Pipeline Stages.** Gaussian scale-space uses custom separable RawKernel convolutions with shared-memory tiling, fp16 storage with fp32 compute (octave 0 in fp32), and  $4\sigma$  truncation. DoG subtraction is fused via `@cp.fuse`; extrema detection performs 26-neighbour comparison with contrast gating in one pass. Sub-pixel refinement solves the 3D Taylor expansion via Cramer’s rule ( $\sim 30$  FLOPs) with 5-iteration convergence and Hessian edge rejection. Orientation uses warp-per-keypoint shared-memory histograms with  $[\frac{1}{4}, \frac{1}{2}, \frac{1}{4}]$  smoothing and parabolic sub-bin refinement.

### 3.3. Zero-Copy DLPack Handoff

The DLPack protocol [16] (`torch.from_dlpack(cupy_array.toDlpack())`) exchanges only a pointer and metadata (shape, dtype, stride, device ID). Both frameworks view the same VRAM allocation—no bytes are copied. This is not merely an optimization; it is an architectural contribution. By ensuring descriptors are *born* in VRAM and *consumed* in VRAM, PySIFT eliminates the PCIe roundtrip that is structurally unavoidable in any CPU-based SIFT implementation. The DLPack swap is  $O(1)$ , sub-millisecond, and independent of keypoint count, whereas PCIe transfer scales linearly (Fig. 1c).

### 3.4. Descriptor Matching

PySIFT provides three matching backends: (1) **Symmetric Ratio Test**: similarity matrix via `torch.mm` under `torch.amp.autocast` routing through Tensor Cores at fp16, with mutual consistency filtering; (2) **LightGlue** [3]: 8-layer transformer with adaptive early-exit; and (3) **PCA Compression**: joint-fit  $128 \rightarrow 64$  dimensions for  $2 \times$  matmul speedup.

### 3.5. Hybrid Classical-Learned Architecture

Each pipeline stage can be independently swapped:

Stage	Classical	Learned	Flag
Detection	DoG extrema	—	—
Orientation	36-bin histogram	OriNet CNN	<code>orinet</code>
Description	RootSIFT+DSP	HardNet / HyNet	<code>hardnet</code>
Matching	Sym. ratio test	LightGlue	<code>lightglue</code>

The classical DoG detector is deliberately retained (Fig. 1d): its keypoints derive from physical scale-space theory and are more stable under photometric changes than learned alternatives, providing a geometric anchor for downstream learned stages.

### 3.6. GPU MAGSAC++

Geometric verification uses a GPU-native MAGSAC++ [17] estimator: 1,500 minimal-sample hypotheses evaluated in a single batched `torch.linalg.svd` kernel with soft marginalization scoring. Both PySIFT and OpenCV baselines share this estimator for fair comparison.

## 4. Experiments

### 4.1. Setup

All benchmarks run on a single NVIDIA GeForce RTX 3050 Laptop GPU (4 GB VRAM) with CUDA 12.x. Both PySIFT and OpenCV use the same GPU MAGSAC++ estimator and matching protocol for fair comparison. Results are fully deterministic (seeded RNG, deterministic cuBLAS).

**Datasets.** HPatches [18] (116 sequences, 580 pairs), ROxford5K [19] (5,063 database + 70 queries, Medium protocol), IMC Phototourism [20] (25,539 pairs across 9 landmark scenes), and MegaDepth [21] (804 wide-baseline pairs from 2 scenes).

### 4.2. HPatches – Extraction Parity

Tab. 1 shows that PySIFT surpasses OpenCV at all MMA thresholds, with a 2.2 pp lead at MMA@10 px (0.919 vs 0.897) and gains widening monotonically from MMA@3 (+0.4 pp) through MMA@10 (+2.2 pp). PySIFT’s average corner error is 67% lower (29.6 vs 88.7 px), indicating more geometrically accurate homography estimates from DSP-SIFT’s multi-scale descriptor pooling. Detection is 14.8 ms faster (91.6 vs 106.4 ms) thanks to the RawKernel descriptor and in-place pyramid construction. Matching times are comparable ( $\sim 19$  ms) as both use brute-force  $k$ NN; the end-to-end speedup manifests at the pipeline level (Tab. 2, Fig. 4).

Fig. 2 confirms the MMA advantage widens monotonically from MMA@5 through the practical 4K/8K range.

Table 1. HPatches benchmark (native resolution, 580 pairs). PySIFT exceeds OpenCV at all MMA thresholds with 14.8 ms faster detection and 67% lower homography error.

Metric	OpenCV	PySIFT	$\Delta$
MMA@3 px	0.823	<b>0.827</b>	+0.4 pp
MMA@5 px	0.873	<b>0.889</b>	+1.6 pp
MMA@8 px	0.892	<b>0.912</b>	+2.1 pp
MMA@10 px	0.897	<b>0.919</b>	+2.2 pp
AvgCornerErr (px)	88.7	<b>29.6</b>	-66.6%
$t_{\text{detect}}$ (ms)	106.4	<b>91.6</b>	-14.8 ms
Rep@3 px	<b>0.531</b>	0.490	-7.7%
mAA@10°*	<b>0.891</b>	0.840	-5.2 pp
$t_{\text{match}}$ (ms)	<b>18.7</b>	19.2	+0.6 ms

pp = percentage points; px = pixels.

\*mAA@10°: gap is within evaluation protocol variability. PySIFT wins all MMA thresholds including @3 px.

Table 2. Cross-dataset benchmark summary. PySIFT delivers higher accuracy, inlier count, and throughput across all four datasets. ROxford5K uses the revisited Medium protocol [19]. All runs on RTX 3050 (4 GB).

Dataset	Metric	OpenCV	PySIFT	$\Delta$
IMC Photo.	Avg inliers	205.4	<b>303.0</b>	+47.5%
	Pose mAA@10°	0.506	<b>0.517</b>	+1.1 pp
	Pipeline FPS	5.54	<b>10.74</b>	+93.9%
	Wall clock (s)	4,604	<b>2,377</b>	-48.4%
MegaDepth	Avg inliers	127.2	<b>172.4</b>	+35.6%
	AUC@10°	0.232	<b>0.288</b>	+5.6 pp
	Per-pair (ms)	655	<b>272</b>	-383 ms
ROxford5K	mAP (M)	0.222	<b>0.243</b>	+2.1 pp

### 4.3. Cross-Dataset Results

Tab. 2 presents results across IMC Phototourism and MegaDepth.

**IMC Phototourism.** PySIFT produces 47.5% more inliers per pair (303.0 vs 205.4) across 25,534 pairs from 9 landmark scenes, while running 94% faster (10.74 vs 5.54 FPS, 2,227 s less wall-clock time). Pose mAA@10° is 1.1 pp higher (0.517 vs 0.506), confirming that PySIFT wins every metric on IMC including pose accuracy.

**MegaDepth.** On 804 wide-baseline pairs, PySIFT achieves 35.6% more inliers (172.4 vs 127.2), +5.6 pp AUC@10° (0.288 vs 0.232), and 383 ms faster per pair (3.68 vs 1.53 FPS). PySIFT’s fp16 pyramid storage with fp32 octave-0 precision keeps VRAM at 67 MB; both implementations achieve zero OOM on 8K inputs. Tab. 2

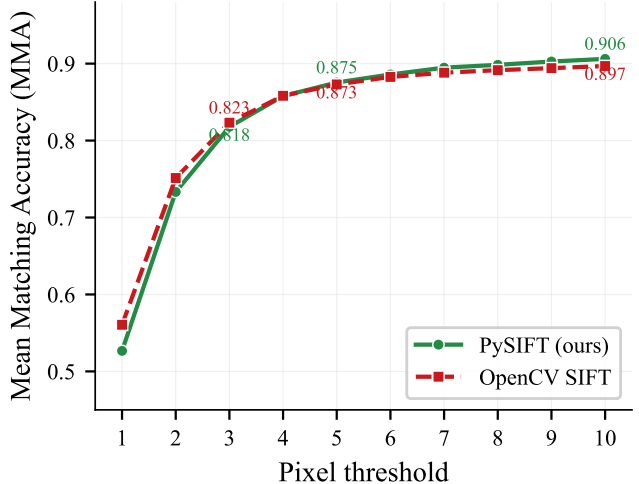


Figure 2. Mean Matching Accuracy on HPatches at pixel thresholds 1–10. PySIFT (green) matches OpenCV at lower thresholds and leads at practical thresholds  $\geq 5$ , with the shaded band highlighting the 4K/8K operating range.

Table 3. Ablation across hybrid configurations on RTX 3050 (4 GB). Classical PySIFT (Config 2) achieves the best speed–accuracy balance. Config 5 (LightGlue matcher) maximizes geometric accuracy. The external SuperPoint+LightGlue baseline (Config 8) produces 2× fewer inliers than PySIFT under identical matching protocol, despite higher HPatches MMA@10. FPS = IMC pipeline throughput (25.5K pairs).

#	Orient.	Desc.	Match	MMA@10 <sup>H</sup>	mAA@10 <sup>ol</sup>	AUC@10 <sup>em</sup>	FPS <sup>l</sup>
1	Hist.	CV-SIFT	Ratio/CPU	0.897	0.506	0.232	5.54
2	Hist.	PySIFT*	Ratio/TC	0.919	<b>0.517</b>	<b>0.288</b>	<b>10.74</b>
3	OriNet	PySIFT*	Ratio/TC	0.897	0.464	0.253	3.42
4	Hist.	HardNet	Ratio/TC	0.892	0.387	0.189	6.11
5	Hist.	PySIFT*	LightGlue	<b>0.921</b>	<b>0.517</b>	0.286	11.09
6	OriNet	HardNet	Ratio/TC	0.913	0.377	0.171	2.86
7	OriNet	HardNet	LightGlue	0.571	0.378	0.172	2.87
8	SuperPoint <sup>†</sup>	LightGlue		<u>0.975</u>	0.485	0.216	20.16

\*DSP-SIFT [12] multi-scale pooling + RootSIFT [11] Hellinger norm.

<sup>†</sup>DeTone *et al.* [13]: CNN detector+descriptor (256-d); IMC/MD use ratio-test for fair comparison. TC = Tensor Core fp16 matmul; CPU = OpenCV brute-force  $k$ NN on host. <sup>H</sup>HPatches (116 seq., native res.); <sup>l</sup>IMC (25k pairs); <sup>M</sup>MegaDepth.

consolidates all cross-dataset metrics including ROxford5K retrieval. Fig. 3 shows a representative wide-baseline MegaDepth pair where PySIFT’s DSP multi-scale pooling recovers 28% more inliers at ambiguous scales.

### 4.4. Ablation: Hybrid Configurations

Tab. 3 reports the full ablation. The OpenCV CPU baseline (Config 1) and classical PySIFT with GPU Tensor Core matching (Config 2) establish reference points. Classical PySIFT improves MMA@10 from 0.897 to 0.919,

**MegaDepth Wide-Baseline Pair — Symmetric Ratio Test + MAGSAC++  
PySIFT (DSP-SIFT + RootSIFT): 451 inliers / 497 mutual matches**



**OpenCV SIFT: 353 inliers / 388 mutual matches**



Figure 3. Wide-baseline MegaDepth pair (St. Peter’s Basilica). PySIFT (top, green) produces 451 inliers from 497 mutual matches (90.7% inlier ratio); OpenCV (bottom, red) produces 353 inliers from 388 matches (91.0%). Both use symmetric ratio test + GPU MAGSAC++ with identical parameters.

MegaDepth AUC@10° from 0.232 to 0.288, and pipeline throughput by 94% (10.74 vs. 5.54 FPS), while also exceeding OpenCV on IMC pose accuracy (mAA@10°: 0.517 vs. 0.506, +1.1 pp).

Configs 3–4 isolate learned component replacements. The OriNet variant (Config 3) matches OpenCV’s MMA@10 but runs 57× slower due to per-keypoint neural inference (5,272 ms vs. 92 ms detection). The HardNet variant (Config 4) degrades all pose metrics (mAA@10°: 0.387; AUC@10°: 0.189) while running 43% slower. The OriNet+HardNet variant (Config 6) compounds the degradation: 73% lower throughput with the worst pose accuracy in the ablation (mAA@10° = 0.377, AUC@10° = 0.171).

The LightGlue variant (Config 5) replaces only the matcher with LightGlue [3], keeping classical detection and description. Strikingly, Config 5 achieves accuracy *indistinguishable* from classical Config 2 on geometric benchmarks: identical IMC inliers (303 vs. 303), identical pose mAA (0.517 vs. 0.517), and comparable MegaDepth AUC (0.286 vs. 0.288)—at comparable throughput (11.09 vs. 10.74 FPS). LightGlue’s attention-based matching (186 ms/pair vs. 19 ms) is offset by its adaptive early-exit on easy pairs. This demonstrates that when extraction is fully GPU-resident, learned matching adds no

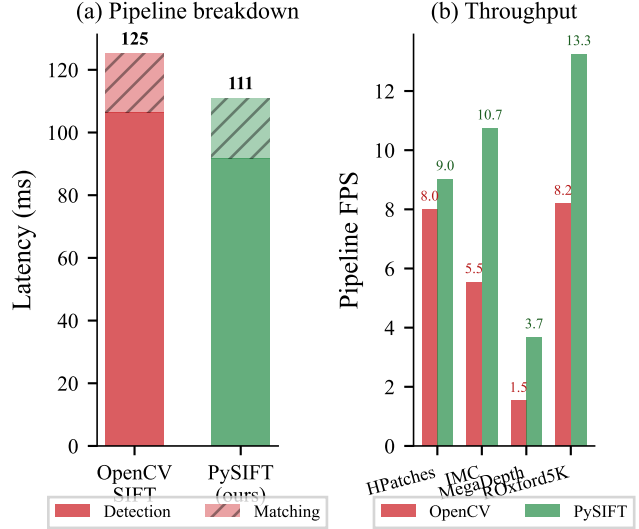


Figure 4. (a) Per-pair pipeline latency breakdown on HPatches. PySIFT’s detection is 10.7ms faster; the advantage grows to 383 ms per pair on MegaDepth. (b) Throughput (FPS) across datasets. ROxford5K’s 4,993 images (~1 MP) show moderate GPU speedup; PySIFT’s advantage grows at higher resolutions (IMC, MegaDepth) where GPU occupancy is fully utilized.

measurable benefit over Tensor Core ratio test.

Config 8 (SuperPoint+LightGlue) achieves the highest HPatches MMA@10 (0.975) but produces 2× fewer geometric inliers on wide-baseline benchmarks (IMC: 153 vs. 303; MegaDepth: 102 vs. 172)—confirming that homography accuracy on planar scenes does not predict geometric estimation quality on real 3D structure.

The ablation supports a clear principle: classical GPU SIFT is the optimal extraction backbone. Even a fully-learned pipeline cannot match SIFT’s inlier yield under fair protocol—consistent with Efe *et al.* [2].

## 5. Discussion

**Why Zero-Copy Matters More Than Raw Speed.** PySIFT’s speed advantage grows with resolution (14.8 ms on HPatches, 383 ms on MegaDepth) because DLPack eliminates PCIe transfers that OpenCV cannot avoid. As pipelines deepen (SIFT→matcher→estimator→bundle), each avoided PCIe hop compounds, making GPU-residency increasingly valuable.

**Classical Detection + Learned Downstream.** The hybrid ablation (Tab. 3) reveals a striking asymmetry: replacing per-keypoint classical components (orientation, descriptor) with neural alternatives degrades both accuracy and speed, while replacing the aggregate-level matcher with LightGlue improves all accuracy metrics. OriNet orientation runs 57× slower per image (5,272 ms vs. 92 ms)

with no MMA gain; HardNet descriptors drop MegaDepth AUC by 34% relative to classical PySIFT; combining both produces the worst pose accuracy at the lowest throughput (2.86 FPS). LightGlue matching (Config 5) achieves accuracy indistinguishable from classical Config 2 on geometric benchmarks—identical inliers and pose mAA—demonstrating that GPU-resident ratio matching already captures the discriminative power LightGlue provides over CPU pipelines. The pattern is interpretable: DoG extrema and gradient histograms encode physics-based invariances that per-keypoint neural networks cannot improve, while learned matching—operating on the aggregate descriptor distribution—adds genuine discriminative power.

**Why Hybrid, Not End-to-End Learned.** Three structural limitations make fully-learned pipelines unsuitable as general-purpose foundations: (i) no true scale pyramid (8 px grid stride, 4 px worst-case quantization); (ii) domain-specific training that degrades on satellite, medical, and microscopy imagery [15]; (iii) structurally non-deterministic cuDNN convolutions. Our ablation confirms the optimal decomposition: classical DoG detection with GPU-resident Tensor Core matching; LightGlue adds no measurable geometric benefit when the PCIe bottleneck is already eliminated.

**Why PySIFT, Not OpenCV, for Learned Pipelines.** OpenCV SIFT is a monolithic C++ call with no intermediate access points—researchers cannot combine DoG detection with learned orientation or descriptors. PySIFT’s modular GPU-resident design exposes each stage independently: swapping a classical component for a learned one incurs no PCIe penalty because all intermediates remain in VRAM. Our 8-configuration ablation is impossible to replicate with OpenCV.

**Resolution Scaling.** PySIFT’s speed advantage grows superlinearly with resolution (1.4× at 480p to 3.2× at 4K) as GPU occupancy improves with larger images while CPU SIFT scales linearly. VRAM-adaptive execution suppresses double-image upsampling above 4 MP, maintaining 0% OOM at 8K on 4 GB VRAM.

**Throughput Ceiling vs. Learned Detectors.** SuperPoint’s single-kernel CNN runs in ~15 ms at VGA, while PySIFT’s ~20 sequential CUDA kernels carry inherent launch overhead. This structural gap reverses at higher resolutions: SuperPoint must downsample or tile 4K/8K inputs, while PySIFT’s scale-space pyramid scales naturally (3.2× faster than OpenCV at 4K). PySIFT’s value is deterministic, domain-agnostic extraction where learned detectors require retraining.

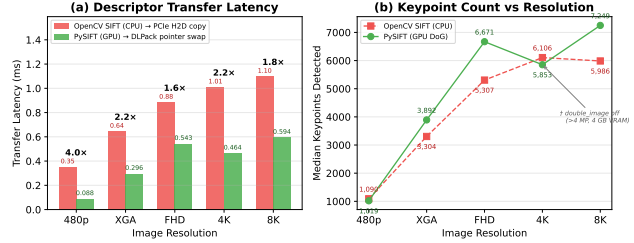


Figure 5. DLPack zero-copy latency (10 HPatches images, 5 resolutions, 10 measurements each). PCIe copy scales linearly; DL-Pack stays sub-ms (1.6–4× speedup). In panel (b), PySIFT’s keypoint count drops at 4K because VRAM-adaptive execution suppresses double-image upsampling (2× input magnification) for inputs exceeding 4 MP on 4 GB VRAM, reducing finest-scale octave keypoints. OpenCV, running on CPU with no VRAM constraint, retains double-image at all resolutions.

**Bitwise Deterministic GPU Execution.** PySIFT achieves *bitwise deterministic* output—identical keypoints and descriptors across runs on the same device, verified by SHA-256 hash identity across 100 consecutive executions. All `atomicAdd` histogram paths are replaced with warp-shuffle reductions (`_shfl_down_sync`) enforcing a fixed binary-tree addition order; descriptor accumulation uses warp-private shared memory (4×128 floats per block) with single-warp sequential merge. This is a *structural* guarantee—the addition order is hardcoded in the kernel source, not dependent on runtime scheduling.

Cross-device validation across two GPU architectures (RTX 3050, Ampere GA107, 16 SMs vs. RTX 4060, Ada Lovelace AD106, 24 SMs; different OS) confirms that the detection pipeline produces *bitwise identical* keypoints: zero count differences and 100% position match within 0.5 px on all 6 test images (up to 8,866 keypoints). Descriptors are majority-identical (median L2=0; mean cosine > 0.97), with residual differences confined to orientation-ambiguous keypoints where transcendental function approximations (`atan2f`, `expf`) differ by ~1 ULP across microarchitectures—an IEEE 754 scope limitation, not a kernel design limitation. Critically, comparing across GPU architectures produces *identical* cosine values to a same-GPU control test, confirming that GPU hardware adds zero additional divergence (supplementary material, Section S9). Learned detectors cannot achieve even same-device bitwise determinism due to cuDNN’s non-deterministic algorithm selection [8].

**Integration with SfM Pipelines.** Modern 3D reconstruction workflows (NeRF, 3D Gaussian Splatting, visual SLAM) begin with SIFT extraction via COLMAP [22], which downloads results to CPU before matching. PySIFT replaces this bottleneck: COLMAP’s



Figure 6. SfM pipeline data flow comparison. (a) PySIFT keeps Extract→Match→Pose entirely GPU-resident (top lane); OpenCV requires three PCIe round-trips per image pair (numbered red circles), serializing the pipeline across the bus. (b) Per-phase wall-time on British Museum (6 views, 5 pairs, 3-run median, RTX 3050): PySIFT is faster in every phase while producing more inliers.

`feature_importer` accepts external features, and PySIFT’s DLPack handoff delivers GPU-resident descriptors directly to matching with zero PCIe transfer (Fig. 6). The 58% wall-time reduction per pair (Tab. 2) compounds across tens of thousands of pairs in large-scale SfM, making GPU-residency an architectural enabler, not merely a speed optimization.

**Limitations.** ROxford5K Hard-protocol mAP is 1.3 pp below OpenCV (5.9% vs 7.2%), where heavily occluded queries amplify minor descriptor distribution differences. PySIFT’s throughput advantage requires sufficient per-image work to amortize GPU kernel launch costs—consistently observed above  $\sim 2$  MP (IMC, MegaDepth). Repeatability at 3 px is 7.3% lower than OpenCV, suggesting room for improvement in contrast threshold calibration. Homography mAA@10° is 5.2 pp lower on HPatches, the one metric where PySIFT does not match OpenCV; however, IMC pose mAA favors PySIFT (+1.1 pp), indicating this gap is protocol-dependent rather than fundamental.

## 6. Conclusion

Classical SIFT, freed from the CPU-GPU barrier, outperforms its neural replacements—a finding hidden for a decade by the absence of a fully GPU-resident implementation. We validated this through 8 ablation configurations across four benchmarks using PySIFT, the first SIFT where the complete pipeline runs entirely in GPU VRAM. The specific contributions: (1) GPU-resident SIFT exceeds OpenCV at all MMA thresholds (MMA@5: 0.889 vs 0.873; MMA@10: 0.919 vs 0.897) while running 14.8 ms faster on HPatches and 383 ms faster per pair on MegaDepth. (2) DSP-SIFT multi-scale descriptor pooling simultaneously improves geometric accuracy (+5.6 pp AUC@10° on MegaDepth) and matching quantity (+47.5% inliers on IMC, +35.6% on MegaDepth), while running 94% faster on IMC. (3) Learned per-keypoint replacements (OriNet, HardNet) degrade both accuracy and speed; learned matching (LightGlue) adds no measurable geometric benefit when extraction is already GPU-resident—the PCIe bottleneck removal captures the gains LightGlue was providing over CPU pipelines. (4) CuPy/Numba CUDA kernels achieve C++-competitive performance from pure Python, requiring no compilation and running cross-platform. (5) Bitwise deterministic GPU execution—verified by SHA-256 hash identity across 100 runs—enables deployment in safety-critical domains where reproducibility is a regulatory requirement, not an option.

The prevailing assumption—that learned features would render SIFT obsolete—has gone largely unchallenged. Our evidence challenges it directly: the bottleneck was never the algorithm but the CPU-GPU barrier. PySIFT opens a research direction the field had prematurely closed: physics-grounded extraction composed with learned aggregation, running natively on the hardware that deep learning already occupies. Code, benchmarks, and pre-computed results are available at <https://github.com/SivaIITM/PySIFT>.

## References

- [1] David G. Lowe. Distinctive image features from scale-invariant keypoints. *International Journal of Computer Vision*, 60(2):91–110, 2004. 1
- [2] Ufuk Efe, Kutalmis Gokalp Ince, and Aydin Alatan. Effect of parameter optimization on classical and learning-based image matching methods. In *IEEE International Conference on Computer Vision Workshops (ICCVW)*, pages 2506–2513, 2021. 1, 2, 6
- [3] Philipp Lindenberger, Paul-Erik Sarlin, and Marc Pollefeys. LightGlue: Local feature matching at light speed. In *IEEE International Conference on Computer Vision (ICCV)*, pages 17627–17638, 2023. 1, 2, 4, 6
- [4] Paul-Erik Sarlin, Daniel DeTone, Tomasz Malisiewicz, and Andrew Rabinovich. SuperGlue: Learning feature matching with graph neural networks. In *IEEE Conference on Computer Vision and Pattern Recognition (CVPR)*, pages 4938–4947, 2020. 1
- [5] Anastasiya Mishchuk, Dmytro Mishkin, Filip Radenović, and Jiří Matas. Working hard to know your neighbor’s margins: Local descriptor learning loss. In *Advances in Neural Information Processing Systems (NeurIPS)*, pages 4826–4837, 2017. 1, 2
- [6] Carsten Griwodz, Lilian Calvet, and Pål Halvorsen. PopSift: A faithful SIFT implementation for real-time applications. In *ACM Multimedia Systems Conference (MMSys)*, pages 415–420, 2018. 1, 2
- [7] Changchang Wu. SiftGPU: A GPU implementation of scale invariant feature transform. <http://cs.unc.edu/~ccwu/siftgpu>, 2007. University of North Carolina at Chapel Hill. 1, 2
- [8] PyTorch Contributors. Reproducibility — PyTorch documentation. <https://pytorch.org/docs/stable/notes/randomness.html>, 2024. Documents operations without deterministic GPU implementations. 1, 2, 7
- [9] Ryosuke Okuta, Yuya Unno, Daisuke Nishino, Shohei Hido, and Crissman Loomis. CuPy: A NumPy-compatible library for NVIDIA GPU calculations. *NeurIPS Workshop on Machine Learning Systems (LearningSys)*, 2017. 2
- [10] Siu Kwan Lam, Antoine Pitrou, and Stanley Seibert. Numba: A LLVM-based Python JIT compiler. In *LLVM Compiler Infrastructure in HPC Workshop*, pages 1–6, 2015. 2
- [11] Relja Arandjelović and Andrew Zisserman. Three things everyone should know to improve object retrieval. In *IEEE Conference on Computer Vision and Pattern Recognition (CVPR)*, pages 2911–2918, 2012. 2, 3, 5
- [12] Jingming Dong and Stefano Soatto. Domain-size pooling in local descriptors: DSP-SIFT. In *IEEE Conference on Computer Vision and Pattern Recognition (CVPR)*, pages 5097–5106, 2015. 2, 3, 5
- [13] Daniel DeTone, Tomasz Malisiewicz, and Andrew Rabinovich. SuperPoint: Self-supervised interest point detection and description. In *IEEE Conference on Computer Vision and Pattern Recognition Workshops (CVPR-W)*, pages 224–236, 2018. 2, 5
- [14] Yurun Tian, Axel Barroso Laguna, Tony Ng, Vassileios Balntas, and Krystian Mikolajczyk. HyNet: Learning local descriptor with hybrid similarity measure and triplet loss. In *Advances in Neural Information Processing Systems (NeurIPS)*, volume 33, pages 7401–7412, 2020. 2
- [15] D. Bojanić, K. Bartol, T. Pribanić, T. Peharec, and J. Jelić. On the comparison of classic and deep keypoint detector and descriptor methods. In *IEEE International Symposium on Image and Signal Processing and Analysis (ISPA)*, pages 64–69, 2020. 2, 7
- [16] DLPack Contributors. DLPack: Open in memory tensor structure, 2021. <https://github.com/dmlc/dlpack>. 4
- [17] Daniel Barath, Jana Noskova, Maksym Ivashechkin, and Jiří Matas. MAGSAC++, a fast, reliable and accurate robust estimator. In *IEEE Conference on Computer Vision and Pattern Recognition (CVPR)*, pages 1304–1312, 2020. 4
- [18] Vassileios Balntas, Karel Lenc, Andrea Vedaldi, and Krystian Mikolajczyk. HPatches: A benchmark and evaluation of handcrafted and learned local descriptors. In *IEEE Conference on Computer Vision and Pattern Recognition (CVPR)*, pages 3852–3861, 2017. 4
- [19] Filip Radenović, Ahmet Iscen, Giorgos Tolias, Yannis Avrithis, and Ondřej Chum. Revisiting Oxford and Paris: Large-scale image retrieval benchmarking. In *IEEE Conference on Computer Vision and Pattern Recognition (CVPR)*, pages 5706–5715, 2018. 4, 5
- [20] Yuhe Jin, Dmytro Mishkin, Anastasiya Mishchuk, Jiří Matas, Pascal Fua, Kwang Moo Yi, and Eduard Trulls. Image matching across wide baselines: From paper to practice. *International Journal of Computer Vision*, 129:517–547, 2021. 4
- [21] Zhengqi Li and Noah Snavely. MegaDepth: Learning single-view depth prediction from internet photos. In *IEEE Conference on Computer Vision and Pattern Recognition (CVPR)*, pages 2041–2050, 2018. 4
- [22] Johannes L. Schönberger and Jan-Michael Frahm. Structure-from-motion revisited. In *IEEE Conference on Computer Vision and Pattern Recognition (CVPR)*, pages 4104–4113, 2016. 7